STRESS INTENSITY FACTOR SOLUTIONS FOR PLANAR DEFECTS WITH IRREGULAR BOUNDARIES

R A Smith* and J F Cooper*†

This paper describes a finite element tool which calculates stress intensity factors at points along the boundaries of irregular planar cracks. New meshes can be automatically calculated for a computed new shape. Results for a stepped rectangular slot are satisfactorily compared with values calculated by an alternative method. The results for a problem of practical interest, a thumbnail crack with a protrusion, are discussed.

INTRODUCTION

Cracks in real structures often have irregular boundaries. Any analysis of fracture instability or fatigue development for such a crack, requires a knowledge of the stress intensity factors at all points on the boundaries. If the crack cannot be represented by a simple geometric shape, then the stress analysis needs to be performed numerically. Any growth of the crack will define a new profile, so that any numerical technique used needs to be capable of accommodating this shape change. This paper describes a finite-element program which is capable of this type of analysis.

A DESCRIPTION OF THE METHOD

Figure 1 illustrates the steps involved in our modelling of a planar crack subjected to Mode I loading. At a number of different positions along the existing crack front, the displacements behind the crack tip are calculated on a plane both normal to the plane of the crack and to the local crack profile tangent. The opening mode stress intensity factor, K_I, at each location is calculated

*Cambridge University Engineering Department
†Now with Mirrlees Blackstone, Stockport, UK

from the standard near crack tip displacement relationships for linear elastic fracture mechanics. For fatigue loading, this local stress intensity factor can be related to a local growth rate through knowledge of the material's fatigue crack growth characteristics. Assuming that the rate remains constant over a number of cycles, the corresponding growth vector normal to the existing crack front can then be calculated for all positions along the crack. The tips of such vectors define a new crack front. The finite element mesh is then reformed around this new front and the whole process can then be repeated.

Details of the Finite Element Model

A 2-D representation of a planar crack was modelled using the MARC system, with the MENTAT mesh generation program. A purpose written program then expanded the 2-D elements into 20-noded rectangular prism elements. To refine accuracy near the crack front, elements along the 2-D crack front were further subdivided into 3-D triangular prisms, with the mid-side nodes surrounding the crack tip automatically set at quarter point positions. Elements away from the crack tip were expanded to rectangular prisms and the resulting 'block' of elements was fitted into a larger block, on the boundaries of which the symmetry and external loading of the problem under consideration were represented. This larger block remained unchanged throughout the problem, whilst the crack front block was automatically remeshed after each calculation of crack shape change.

Comparison with Known Results

It is vital that the results from any finite element calculation are compared with known values, before the system is 'let loose'. To achieve this, the stepped rectangular slot of Fig. 2 was analysed. The crack was symmetrical about the centre line shown, and subjected to uniform remote stress. The calculated values of K_I (plane strain), are compared with values calculated by Murakami [1] using a body force method. The comparison is excellent and lends confidence to our technique. It is immediately apparent that re-entrant corners, such as C, have high values of K, whilst constrained corners such as D and B have much lower values. The nature of the stress singularities at C, D and B, together with that at the intersection of the crack front with the free surface, E, is a topic of current debate. It is unlikely that the well known $(r)^{-\frac{1}{2}}$ crack singularity is valid at these points; this will be discussed in further publications. However, it is apparent that once profile smoothing occurs, this nicety is of little practical importance. That smoothing will indeed occur is obvious because the local growth vectors at the higher values of K (E, C, A) will be larger than those at the constrained corners (D, B).

FATIGUE DEVELOPMENT OF STEPPED SLOT DEFECT

Figure 3 shows successive profiles calculated using a growth law of the type $da/dN \propto \Delta K^{2.92}$, an exponent typical of an offshore structural steel. The lives are presented as a dimensionless ratio of cycles, since absolute values require a particular initial defect size and the constant of proportionality in the growth rate equation above. Note that higher values of the propagation law index would simply hasten the profile smoothing process. Also shown in Fig. 3 is the ratio of the maximum K values of the profile to the minimum value: a ratio which decreases towards iso-K as the crack shape smooths.

THUMBNAIL CRACK WITH A PROTRUSION

Figure 4 illustrates a thumbnail (elliptical) crack with a protrusion at its region of deepest penetration into the material. We term this the 'nipple' profile. Bounding ellipses for this shape are also shown; these shapes were used to compare our finite element K values, with results published by Newman and Raju [2]. Although not quoted here, satisfactory agreement was obtained, thus further confirming our techniques. This geometry is of practical importance because of the method of simplifying complex defects by using encompassing ellipses, suggested in current defect safety assessment codes (e.g. ASME, XI [3] and PD 6493 [4]). The immediately surprising result is that the K value at the point of deepest penetration of the protrusion (A), drops to a considerably lower value than that of the bounding ellipses; whilst that at the intersection of the protrusion and the parent ellipse has a much enhanced value. As far as fracture stability is concerned, this means that unless the protrusion occupies a large proportion of the existing crack front, it is mechanically stable. The fatigue development, calculated in the same manner as before, is shown in Fig. 5, together with further evidence to illustrate the strong drive towards an iso-K configuration as the profile develops, i.e. $K_{max}/K_{min} \to 1$ as the profile smooths.

CONCLUDING REMARKS

This paper has described a technique for calculating the shape development of planar cracks subjected to Mode I loading. The finite element method used automatically recalculates a new mesh to suit a developed profile. The important practical case of a protrusion on a thumbnail defect has been analysed and has been shown (for a small protrusion) to be mechanically stable. The method can be extended to cover cases of interacting planar defects and internal defects. This work is now underway.

ACKNOWLEDGEMENTS

Thanks for financial support from the Marine Technology Directorate of SERC and UKAEA (Risley), together with thanks to MARC Analysis for the use of their program, are gratefully made.

REFERENCES

[1] Murakami, Y, Personal communication, 1986

[2] Newman, J C and Raju, I S, Engng. Fract. Mech., Vol. 15, 1981, pp. 185-192

[3] ANSI/ASME Boiler and Pressure Vessel Code, Section XI, American Society of Mechanical Engineers, 1986

[4] PD 6493, Guidance on some methods for the derivation of acceptance levels for defects in fusion welded joints, British Standards Institution, 1980

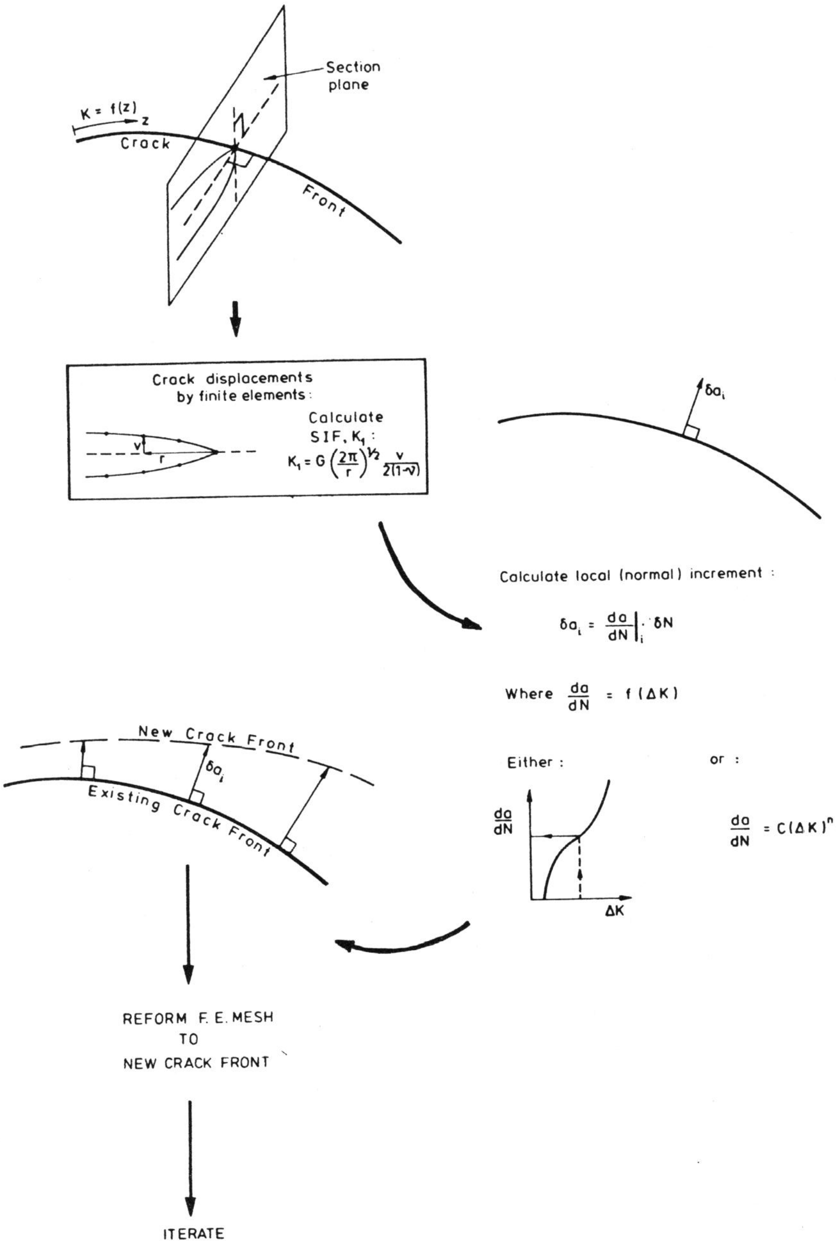

Figure 1 Modelling the growth of K varying crack fronts by FEM

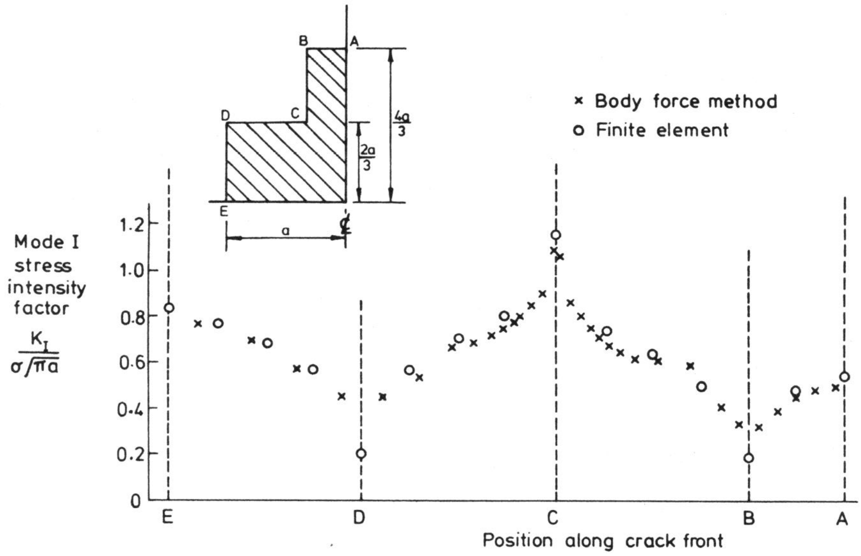

Figure 2 K_I results for a stepped defect by FEM and Body Force [1] methods ('a' lies on a free surface)

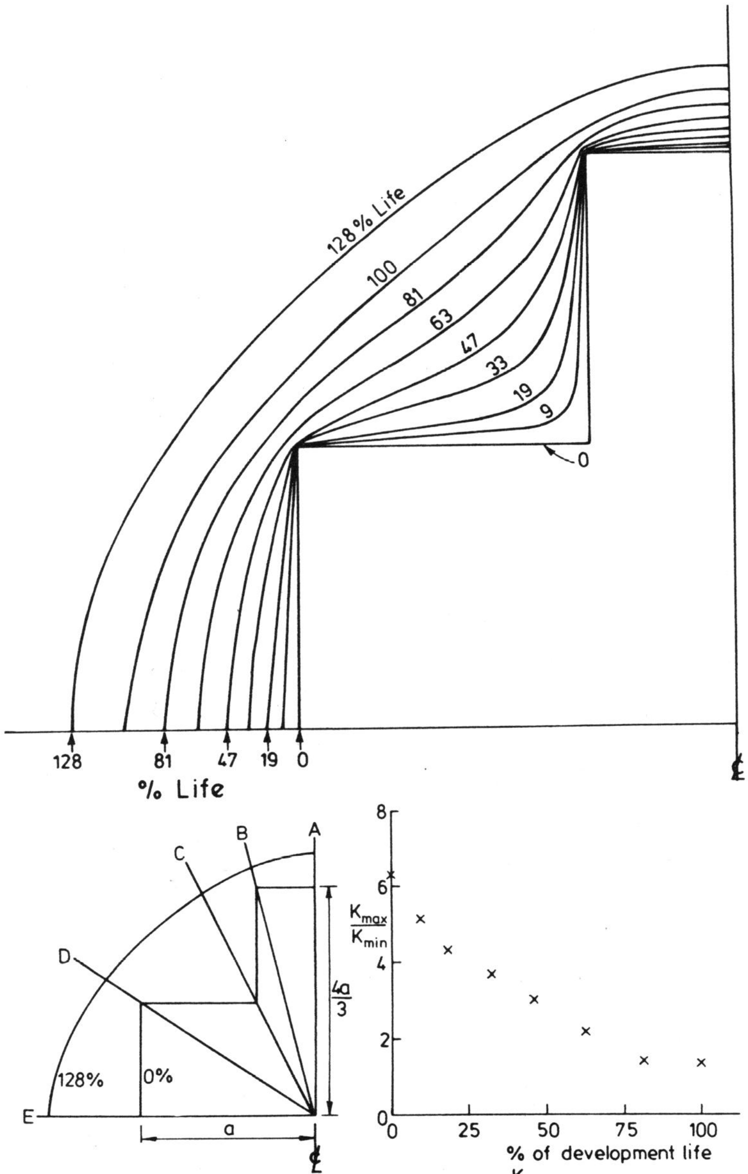

(a) Change of $\frac{K_{max}}{K_{min}}$ along crack from as effect of the sharp corners diminish.

Figure 3 Fatigue development of a stepped slit

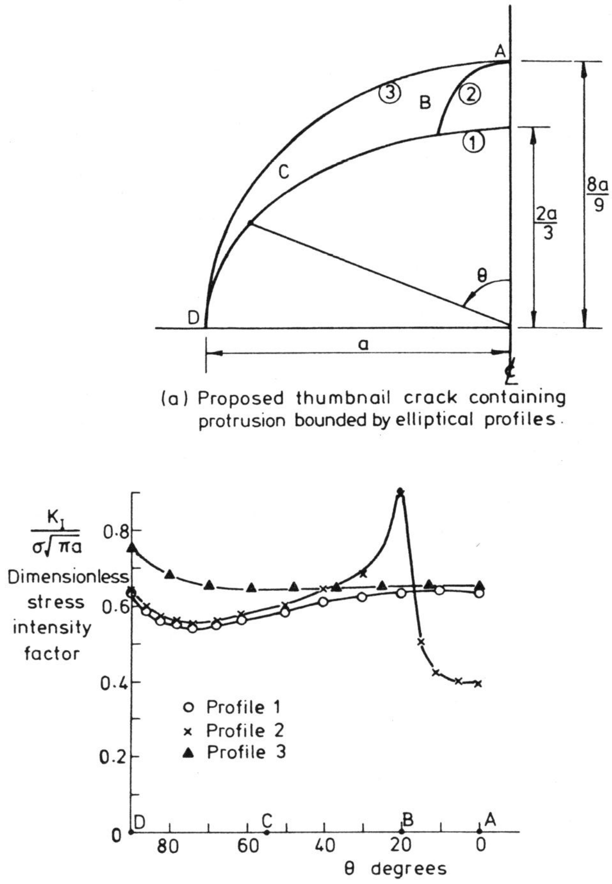

(a) Proposed thumbnail crack containing protrusion bounded by elliptical profiles.

(b) Variation of stress intensity factors along crack fronts.

Figure 4 The 'nipple' profile and resulting K_I values ('a' lies on a free surface)

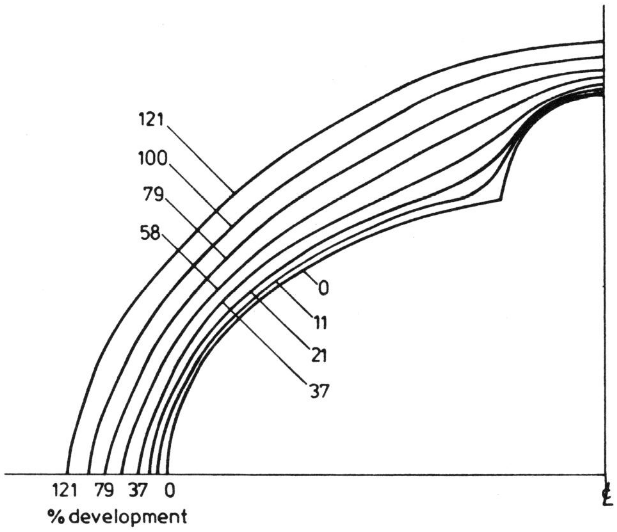

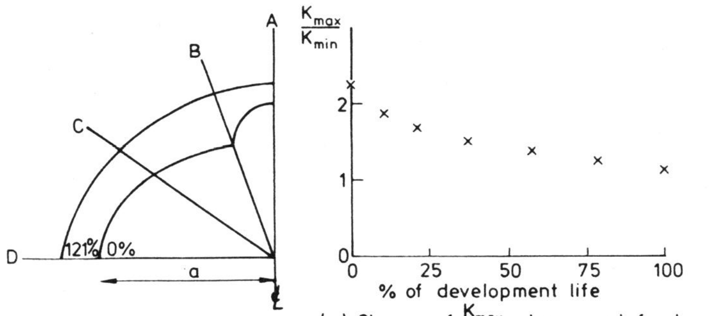

Figure 5 Fatigue development of the nipple profile